Iranian Journal of Materials Forming 6 (1) (2019) 32-43

Online ISSN: 2383-0042

IJMF

Iranian Journal of Materials Forming

Journal Homepage: http://ijmf.shirazu.ac.ir

Plastic Deformation Characteristics of Continuous Confined Strip Shearing Process Considering the Deformation Homogeneity and Damage Accumulation

M. Shaban Ghazani*

Department of Materials Science Engineering, University of Bonab, Bonab, Iran

ARTICLE INFO

Article history:

Received 26 June 2018
Revised 27 December 2018
Accepted 3 January 2019

Keywords:

Finite element analysis
C2S2 process
Strain homogeneity
Damage accumulation

ABSTRACT

In the present investigation, two dimensional elastoplastic finite element analysis was conducted to assess the deformation characteristics of Al 1100 alloy during continuous confined strip shearing (C2S2) process. The results of simulations showed that the plastic strain distribution across the deformed sample is non-uniform irrespective of the amount of friction and C2S2 die angle. The most uniform distribution of equivalent strain is achieved when the friction coefficient and die angle are equal to 0.3 and 90˚ respectively. It was also observed that the maximum damage factor is located in the inner regions of the cross section of the plate similar to the conventional ECAP processing of soft materials with higher strain hardenability. According to a set of simulations, executed at different frictions and die angles, it was demonstrated that the safest condition is achieved during deformation with a friction coefficient of 0.3 and die angles of 90˚ and 110˚. Besides, the analysis of the equivalent strain rate pattern showed that the width of the deformation zone decreases by increasing the friction coefficient and decreasing the C2S2 die angle.

1. Introduction

The conventional rolling process is widely used for the production of metallic sheets on an industrial scale [1]. In this process, the improved mechanical properties such as tensile and yield strength are achieved only at higher reductions after repeated cycles, which is not cost effective because it requires a series of rolling steps executed using expensive equipment and inter-pass heat treatment [2-4]. Moreover, increase in mechanical properties during rolling is limited because it requires higher thickness reductions which are not possible in the conventional rolling. Therefore, another drawback of the rolling process is the limited grain refinement in metallic sheets due to the limitation in the imposed plastic strain. Intense grain refinement of the microstructure of metallic sheets and plates requires the application of a deformation process in which a severe plastic strain can be applied without considerable thickness reduction. In recent years, numerous severe plastic deformation (SPD) processes such as high pressure torsion [5], accumulative roll bonding [6], constrained groove pressing [7], equal channel angular pressing [8], multidirectional forging [9] and several other newly developed techniques [10-13] have been introduced and used successfully to produce ultra-fine grained and nanostructured materials. Equal channel angular pressing is the most effective and promising technique proposed by Segal [14] to impose shear deformation on metallic materials Fig. 1 (a). In this process, a sample with square or circular cross section is passed through the intersecting area of the two channels with equal cross

* Corresponding author
E-mail addresses: m.shaban@bonabu.ac.ir (M. Shaban)

sections. Iwahashi et al [8] showed that the amount of the imparted strain to the sample, ignoring the effect of friction and material properties such as strain hardening exponent, can be calculated using the following equation:

$$\bar{\varepsilon} = \frac{N}{\sqrt{3}}\left[2cot\left(\frac{\Phi+\Psi}{2}\right) + \Psi cosec\left(\frac{\Phi+\Psi}{2}\right)\right] \quad (1)$$

Where Φ is die angle and Ψ is the outer curvature angle of the intersecting area and N is the number of ECAP passes. The main advantage of ECAP process is that the cross section area of the sample remains constant so that the sample can be removed and repressed into the die channel to impose a higher amount of plastic strain on the material. Although this process is considerably effective in the grain refinement of different metals and alloys and has been used to produce nanostructured materials of different types [15-18], the main disadvantage of this severe plastic deformation method is that only the processing of small workpieces is feasible and the process cannot be performed in a continuous manner to produce nanostructured strip shaped samples. Therefore, Lee et al [19] proposed a new sheet forming technique called continuous confined strip sheering (C2S2) combining the rolling and ECAP processes. The schematic representation of this metal forming process is shown in Fig. 1 (b). In this process, the sheet metal is passed through the ECAP die under the feeding force of the roller, and the shear deformation is applied to the material in the intersecting area of the two channels similar to the conventional ECAP processing. The total effective strain ($\bar{\varepsilon}$) applied to the sheet metal can be calculated using the following expression [20]:

$$\bar{\varepsilon} = \frac{N}{\sqrt{3}}K^2\left[2cot\left(\frac{\Phi+\Psi}{2}\right) + \Psi cosec\left(\frac{\Phi+\Psi}{2}\right)\right] \quad (2)$$

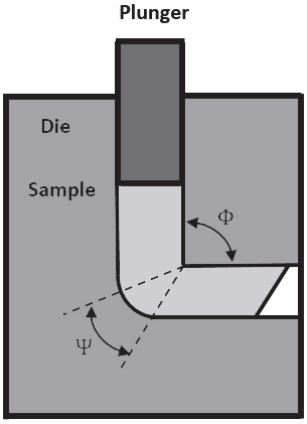

(a)

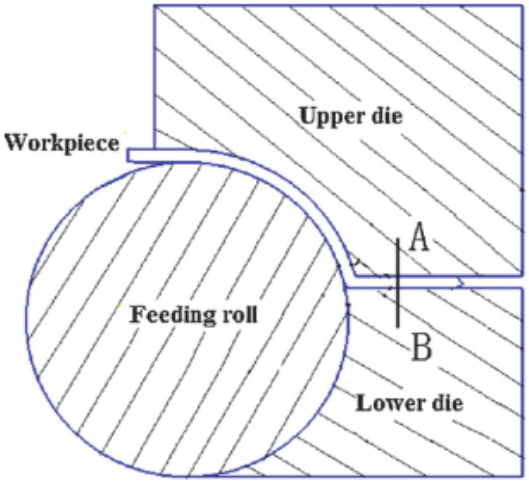

(b)

Fig. 1. Schematic of conventional ECAP (a), C2S2 process (b) [21, 26].

Where Φ is die channel angle, Ψ is outer curvature angle, N is the number of C2S2 passes, and K is the thickness ratio ($K = \frac{H_1}{H_0}$). The open literate search demonstrates that the C2S2 process is an effective severe plastic deformation technique that can be used successfully for the production of ultra-fine grained aluminum strips [19]. Although the deformation characteristics of this process have been studied using finite element analysis [21], there is not any information about the homogeneity of the applied plastic strain and the resultant microstructure as well as the development of the damage in the strip. Therefore, in the present investigation, two-dimensional finite element simulation was conducted to analyze the deformation characteristics of the C2S2 process with an emphasis on the plastic deformation homogeneity and damage development in the samples.

2. Finite Element Analysis

The practical implementation of deformation processes to optimize different process parameters is very time consuming and costly. With respect to this, finite element simulation is an effective and promising tool which can be used successfully to evaluate the flow behavior and deformation characteristics of materials and optimize the complex and experimentally expensive metal forming processes. In this study, two-dimensional finite element simulation was conducted using

DEFORM 2D™ commercial code to analyze the deformation characteristics of the continuous confined strip shearing (C2S2) process. The schematic representation of the simulated C2S2 method is shown in Fig. 2 (a) and the process parameters are listed in table. 1. The dimensions of the initial sheet were selected to be 160 mm × 10 mm and also Al 1100 was chosen as the model material. The feeding rolls with radii of 200 mm were taken as rigid bodies and the strip deformable in the simulation. The friction between the feeding roles and the sample provided a driving force to pass the sheet through the ECAP die channel. Therefore, the friction coefficient between the rollers and the sheet was considered to be 0.9 which was sufficient to push the front part of the sheet in to the ECAP die channel. Besides, the friction between the sample and the ECAP die channel wall provided resistance force against the material flow, which is a disadvantageous factor in the C2S2 process. In the present investigation, this friction was considered to vary within the range of 0-0.3 to assess its effect on the flow behavior of Al1100 material during the C2S2 process. The sample was initially meshed with 1500 four node plane strain elements and automatic re-meshing was used in all the simulations. The deformed meshes of the sample are shown in Fig. 2 (b). Moreover, all the simulations were conducted with a constant roll speed of 0.1 rad/s. Since the isothermal conditions were achieved during low strain rate deformation, the effect of temperature rise was ignored. Different simulations were performed with ECAP die angles within the range of 90-110˚ to analyze the simultaneous effect of the friction coefficient and die angle on the deformation characteristics of the C2S2 process. Besides, the thickness of the sample was considered to be constant during the deformation.

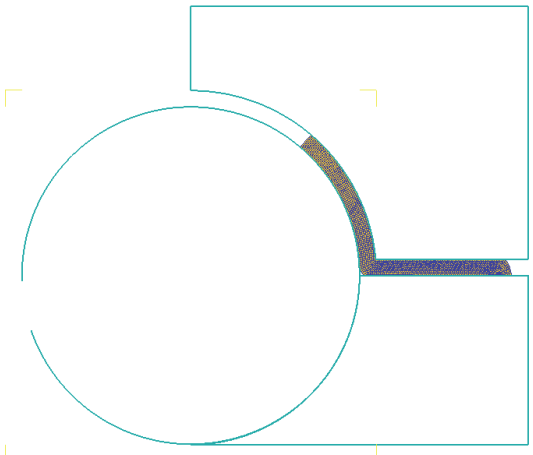

(a)

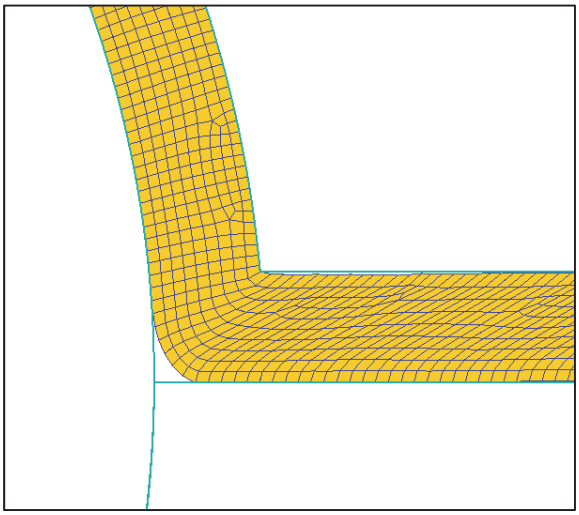

(b)

Fig. 2. Two-dimensional representation of the C2S2 setup used in finite element analysis (a), magnified view of the deformation zone showing the die angle (Φ), outer curvature angle (Ψ), and deformed meshes (b).

3. Results and Discussion

3.1. Plastic strain distribution

Figure 3 shows the distribution of equivalent plastic strain in the deformed plate during the C2S2 process considering a constant die angle of 90˚ and assuming different friction coefficients. It is seen that the plastic strain distribution is not uniform in all conditions and its magnetite is affected by the friction between the samples and die wall. It is obvious that the amount of the equivalent plastic strain increases by increasing friction coefficient at the same locations inside the deformed plate. Besides, the corner gap during the C2S2 process in all friction coefficients (denoted by 'CG' in Fig. 3).

It is worth noting that the corner gap formation is a common feature of the ECAP processing of materials with a high strain hardening capability such as pure aluminum which was selected as the model material in the present investigation. The formation of the corner gap in the intersecting area of ECAP channels reduces the plastic strain imposed on the bottom side of the sample. As it is evident, the amount of the plastic strain at the top side of the plate is higher than that at the bottom regions at all friction coefficients. Careful

inspection of Fig. 3 reveals that the corner gap area decreases by increasing the friction coefficient. Consequently, the width of the area subjected to lower plastic deformation in the bottom regions of the samples decreases by increasing the friction.

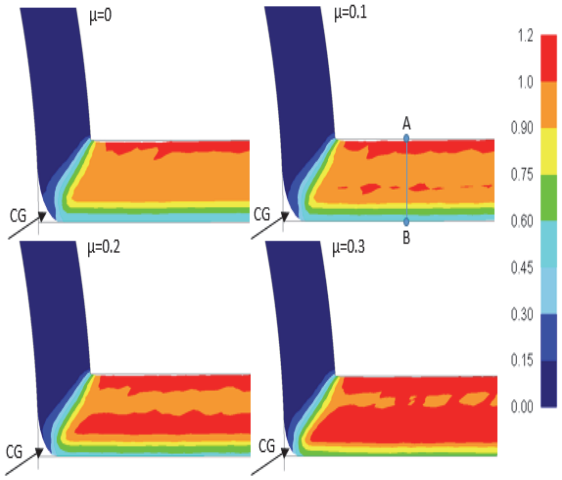

Fig. 3. The effect of friction coefficient on the plastic strain distribution in the deformed plate and also the corner gap formation at a constant die angle of 90˚.

The variations of the equivalent plastic strain across the deformed plate (AB line in Fig. 3) is shown in Fig. 4 As can be seen, at a die angle of 90˚ (Fig. 4 (a)), the amount of the plastic strain increases to a maximum value at a point 7 mm away from the topside of the plate and then decreases to a minimum value at the bottom of the plate. As it is seen, the difference between the equivalent plastic strains of the samples deformed at a die angle of 90˚ is not significant in the upper regions but the sensible difference in the imposed plastic strain is observable in the bottom half of the sample. This is due to the effect of the friction between the surface of the sheet and the die channel wall, which exerts the inverse force in the opposite direction to the material flow and reduces the size of the corner gap in the intersecting area of channels. But, at a channel angle of 110˚, as seen in Fig. 4 (b), the effect of the friction on the plastic strain distribution is negligible compared with that at a die angle of 90˚. It is concluded that the effect of the friction is more pronounced at lower channel angles and that increase in the C2S2 channel angle reduces the effect of the friction coefficient.

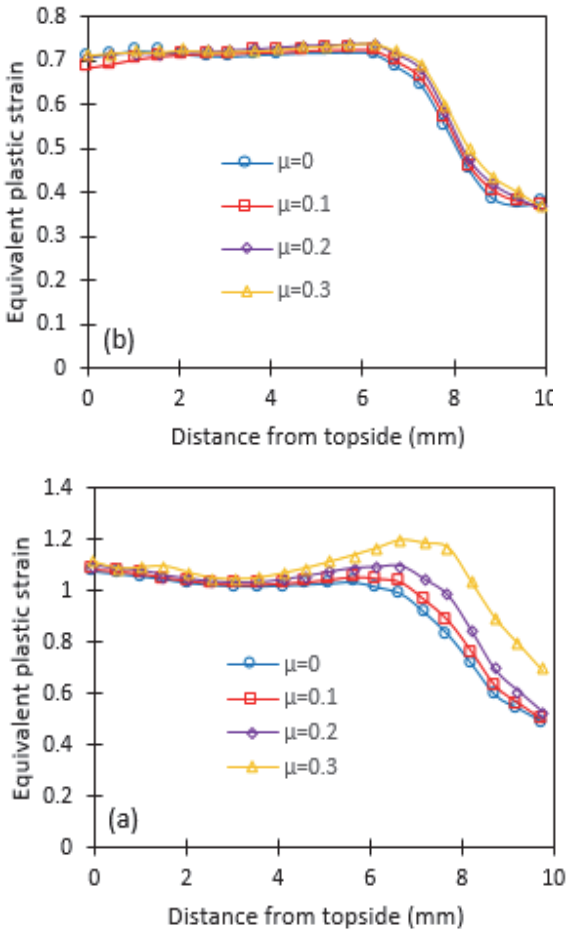

Fig. 4. The effect of friction coefficient on the variations of the equivalent plastic strain across the deformed sample at C2S2 die angle of A) 90˚ and B) 110˚.

The effect of C2S2 die channel angle on the equivalent plastic strain distributions in the deformed plate is represented in Fig. 5 As it is seen, the die channel angle has no significant effect on the distribution pattern of the plastic strain. But the amount of the imposed plastic strain at a specified region decreases by increasing the C2S2 die channel angle. It is also obvious that the extent of the corner gap at the bottom side of the intersecting area remains almost constant and the C2S2 die channel angle has no sensible effect on the corner gap formation. It can also be concluded that the width of the area subjected to lower strains at the bottom side of the plate increases as the C2S2 die channel angle is increased. Fig. 6 represents the variations of the equivalent plastic strain across the deformed plate (AB line depicted in Fig. 5) at constant friction coefficients and varied die channel angles.

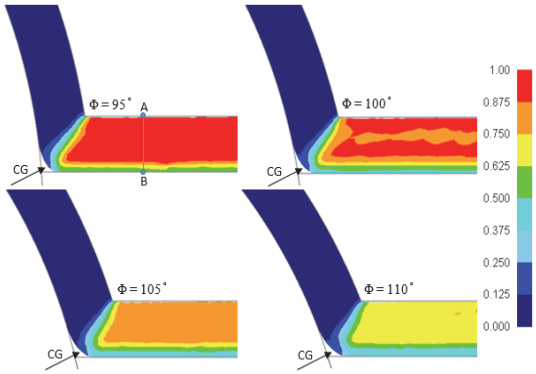

Fig. 5. The effect of the C2S2 die angle () on the plastic strain distribution in plate during processing at a constant friction coefficient of 0.3.

Figure 6 (a) shows the plastic strain variations at frictionless conditions. It can be deduced that the plastic strain at the specified point away from the upside of the sample increases by decreasing the C2S2 die channel angle. Besides, the amount of the plastic strain remains almost constant in the 6 mm of the topside of the thickness of the plate and then decreases continuously up to the bottom side of it. The similar trends are observable when the friction coefficient is selected to be 0.3 according to Fig. 6 (b); however,a minor difference can be noticed by careful inspection of the strain variations in Fig. 6 (a) and Fig.6 (b). In the case of the frictionless conditions as represented in Fig. 6 (a), the amount of the plastic strain in the 6 mm of the topside of the sample is almost constant whereas the plastic strain in the topside of the sample in Fig. 6 (b) decreases to some extent and then increases to its maximum value in the point located 6 mm away from the topside of the plate. This trend is more obvious at low C2S2 die angles in Fig. 6 (b), for example the die angles of 90˚ and 95˚.

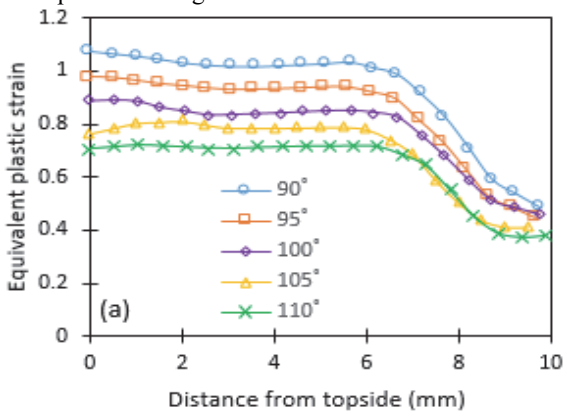

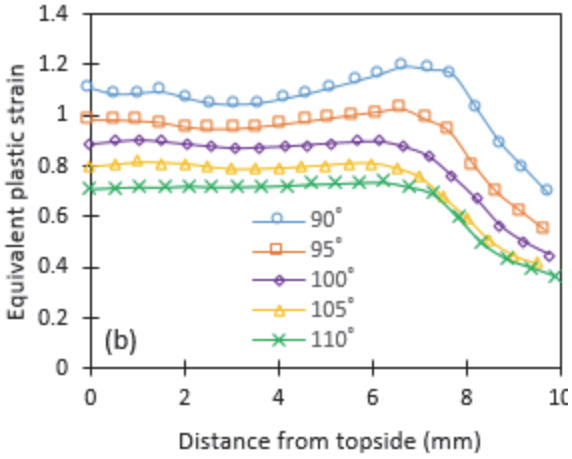

Fig. 6. Variations of the equivalent plastic strain across the deformed sample at different C2S2 die angles: a) at frictionless conditions, b) at friction coefficient of 0.3.

3.2. Homogeneity of plastic deformation

The homogeneity of the equivalent plastic strain imposed on samples during the severe plastic deformation processes greatly influences the microstructure homogeneity of the processed material. Therefore, the evaluation of the homogeneity of plastic deformation is of great importance. For this reason, the value of the coefficient of the variance of the equivalent plastic strain ($CV_{\bar{\varepsilon}}$) can be measured according to the following expression [22]:

$$CV_{\bar{\varepsilon}} = \frac{Stdev(\bar{\varepsilon})}{Avg\ (\bar{\varepsilon})} \qquad (3)$$

Where $Stdev(\bar{\varepsilon})$ is the standard deviation of the plastic strain and $Avg\ (\bar{\varepsilon})$ is the average value of the equivalent plastic strain across the predefined path. In the present investigation, the values of $CV_{\bar{\varepsilon}}$ across the processed plate, as denoted by AB line in Fig. 5, were measured at different die angles ranging from 90 to 110˚ and different friction coefficients in the range of 0 to 0.3 and the resultant contour plot was obtained showing the variations of inhomogeneity index ($CV_{\bar{\varepsilon}}$) with the die channel angle and friction coefficient (Fig. 7). In this plot the higher amounts of $CV_{\bar{\varepsilon}}$ correspond to the higher inhomogeneity in the plastic strain distribution and consequently the more non-uniform microstructure. Inspection of this plot shows that a more uniform microstructure is achieved when the friction coefficient between the plate and die wall is about 0.3 and the C2S2

die channel angle is selected to be 90˚. Besides, a more inhomogeneous plastic strain distribution and the resultant microstructure are obtained in the frictionless condition when the C2S2 die angle is selected to be 95 and 105˚.

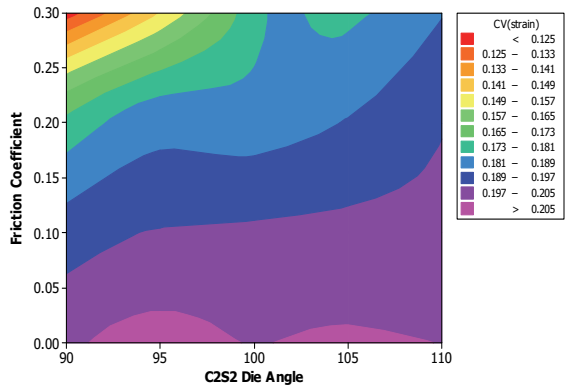

Fig. 7. Contour plot showing the effect of friction coefficient and C2S2 die angle on the strain inhomogeneity factor ($CV_{\bar{\varepsilon}}$) throughout the thickness of the deformed plate.

3.3. Strain rate pattern and the shape of the deformation zone

Figure 8 shows the distribution of the equivalent strain rate in the samples during deformation with a C2S2 die angle of 90˚ considering different values for the friction coefficient. It can be seen that the strain rate value is nonzero only at the intersection area of the channels. The equivalent strain rate is zero at other regions of the plate located before and after the intersection area.

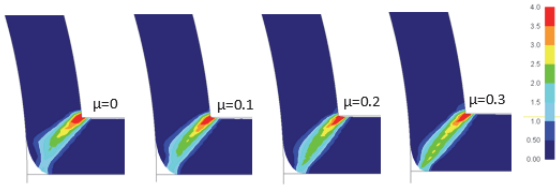

Fig. 8. Strain rate pattern and the deformation zone in the C2S2 process with a die angle of 90˚ at different friction coefficients.

It is also worth noting that the shape of the region with nonzero strain rate represents the shape of the deformation zone. As illustrated in this figure, the plastic deformation is imposed on the sample with a higher strain rate at the inner regions of the intersecting area, while the strain rate is lower at the outer regions. It can also be deduced that the deformation zone becomes narrower by increasing the friction coefficient. The effect of C2S2 die angle (Φ) on the shape of the deformation zone is represented in Fig. 9 It is seen that the width of the deformation zone increases with the increase of the die angle. Moreover, the area with a higher strain rate (denoted by red color) in the inner regions of the intersecting channels decreases by increasing the C2S2 die angle. The variations of the equivalent strain rate on the intersecting plane from inner to outer regions (AB line in Fig. 9) are demonstrated in Fig. 10. It is deduced that the strain rate value decreases from inner to outer regions of the intersecting line (AB line) and at a specified point on AB line, the equivalent strain rate decreases by increasing the C2S2 die angle.

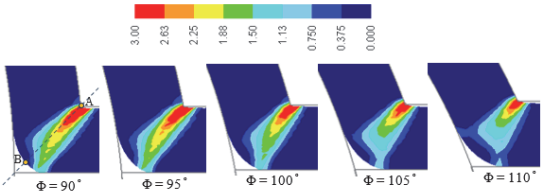

Fig. 9. Strain rate pattern and the shape of the deformation zone at different die angles in frictionless conditions.

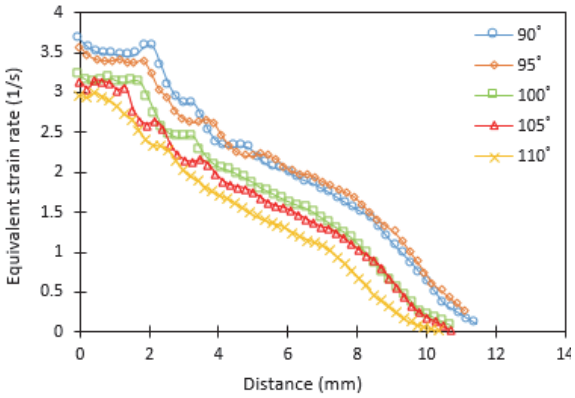

Fig. 10. Variations of the strain rate across the deformed sample from point A to B (as indicated in Fig. 9) at different channel angles.

3.4. Damage accumulation

One of the major problems in the ECAP processing of materials is the formation of superficial cracks at the upper side of the sample, especially in the case of the so called difficult-to-work-with materials such as titanium and magnesium [23-24]. In this case, samples were cracked from the top surface and could not be further processed to achieve higher amounts of the equivalent plastic strain required for the formation of

nanostructured metals. As the C2S2 process is the reversion of the ECAP process, it is probable that the processing of materials with this process is limited by the formation of superficial cracks. In the case of strain hardened materials such as annealed aluminum and its alloys, it has been demonstrated that the maximum damage occurs in the inner regions of the sample which are subjected to compressive stresses that prevent the propagation of the initiated cracks [25]. But there is not any information about the damage development in plates subjected to the C2S2 process. The Craft-Latham damage criterion is usually used to evaluate fracture in severe plastic deformation processes. The Craft-Latham damage can be evaluated using the following expression [26]:

$$C = \int_0^{\varepsilon_f} \frac{\sigma_m}{\bar{\sigma}} d\bar{\varepsilon} \qquad (4)$$

where σ_m is the maximum component of the stress tensor, $\bar{\varepsilon}$ is effective strain, $\bar{\sigma}$ is effective stress, C is a constant indicating the critical condition for the initiation of fracture and the integral is calculated from zero strain to final strain (ε_f). According to Eq (4), cracks are initiated when the amount of the damage factor reaches the critical value. Fig. 11 shows the distribution of the Craft-Latham damage factor in the cross section of the workpiece at different friction coefficients when the C2S2 die angle is considered to be constant (90˚). As can be seen, the friction coefficient does not have any significant effect on the distribution pattern of the Craft-Latham damage inside the deformed plate.

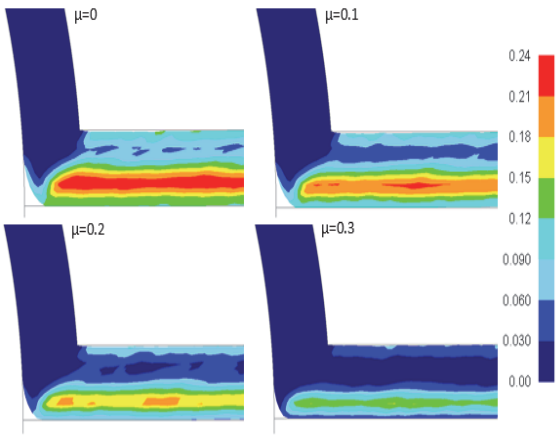

Fig. 11. Simulated Craft-Latham damage distribution in plate during C2S2 processing with a die angle of 90˚ at different friction coefficients.

It is demonstrated that the maximum amount of damage occurs in the inner regions of the cross section of the deformed plate. Besides, the amount of the maximum damage decreases with the increase of the friction coefficient. It is also obvious that the upper and bottom sides of the plate have lower amounts of damage and the formation of superficial cracks is overruled. The effect of the C2S2 die angle on damage distribution in the sample is shown in Fig. 12. It is clear that the distribution pattern of the damage factor does not change with the C2S2 die angle. In all die angles, a higher damage occurs in the inner regions of the deformed plate.

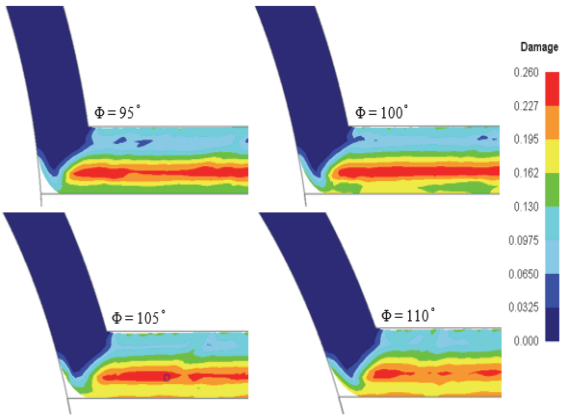

Fig. 12. Simulated Craft-Latham damage distribution in plate during C2S2 processing at different die angles in frictionless conditions.

Figure 13 (a) shows the variation of the Craft-Latham damage across the deformed plate (AB line in Fig. 5) at the constant die angle of 90˚ and different friction coefficients. It is concluded that the amount of the damage factor in the upside, downside and inner regions of the sample decreases by increasing the friction coefficient. Moreiver, the point at which the maximum damage occurs shifts to the bottom side of the sample by increasing the friction coefficient. Besides, inspection of Fig. 13 (b) reveals that the amount of damage in the upper, lower and middle parts of the sample increases by increasing the C2S2 die angle. From above-mentioned statements, it can be concluded that similar to the conventional ECAP processing of annealed materials with higher strain hardenability, the maximum damage occurs in the inner regions of the plate during the C2S2 process and that the formation of superficial cracks can be avoided, but the cracks may initiate from the inside of the plate.

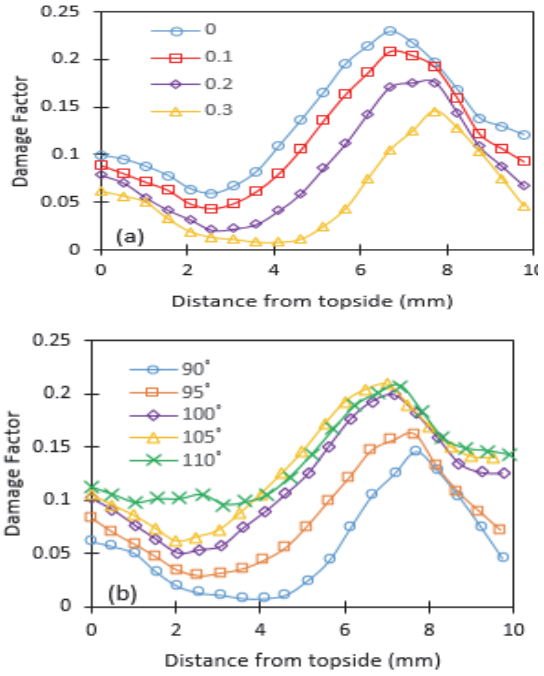

Fig. 13. Variations of the Craft-Latham damage across the deformed sample at a C2S2 die angle of 90˚ (a) and constant friction coefficient of 0.3 (b).

The value of the maximum damage occurring at different conditions was determined and its variations with C2S2 die angle and friction coefficient is shown as a contour plot in Fig. 14. This contour plot demonstrates that regions A and B, corresponding to the friction coefficient of 0.3 and die angles of 90˚ and 110˚ respectively, are the safest conditions to execute the C2S2 process whereas region C corresponding to the frictionless condition and the C2S2 die channel angle in the range of 97.5-105˚ is more prone to the formation of cracks during processing.

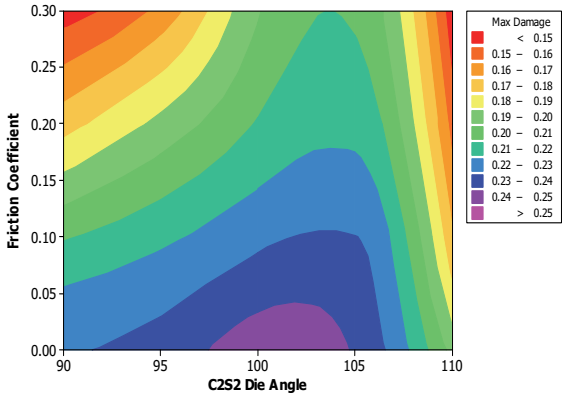

Fig. 14. Contour plot showing the variations of the maximum damage with friction coefficient and C2S2 die angle.

3.5. Torque-time curves

Fig. 15 (a) shows the time history of the torque calculated from the feeding roll at a constant die angle of 90˚ and different friction coefficients. As can be seen, the variations of the calculated torque with time are similar to each other. At first the torque increases rapidly and then remains almost constant and finally decreases continuously at the end of the deformation and reaches to zero when the C2S2 process is stopped. It is seen that the torque value increases by increasing the friction coefficient. In addition, the torque-time curves in Fig. 15 (b) indicate that the magnitude of the torque needed for the execution of the C2S2 process increases by decreasing the C2S2 die angle.

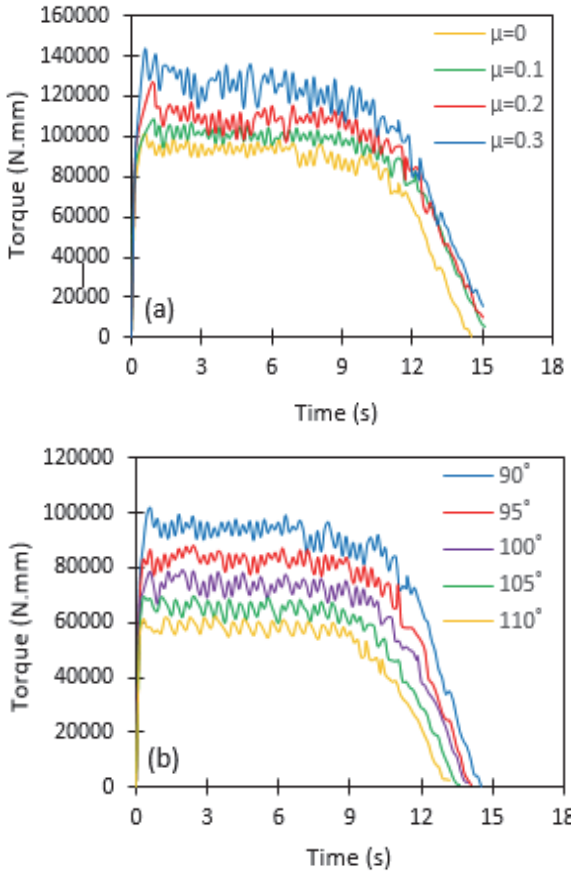

Fig. 15. Variations of the torque with time during the C2S2 process: a) at constant die angle of 90˚showing the effect of the friction coefficient, and b) at a friction coefficient of 0.1 showing the effect of the die angle.

The contour plot showing the variations of the maximum torque with the die angle and friction coefficient is represented in Fig. 16. As it is clear, the maximum torque is required when the die angle and

friction coefficient are 90˚ and 0.3 respectively and the minimum torque corresponds to the deformation with a die angle of 110˚ in the frictionless conditions. It is worth noting that the torque value in the present study was calculated considering the sample width of 10 mm. Therefore, this point must be considered while deforming sheets of different widths.

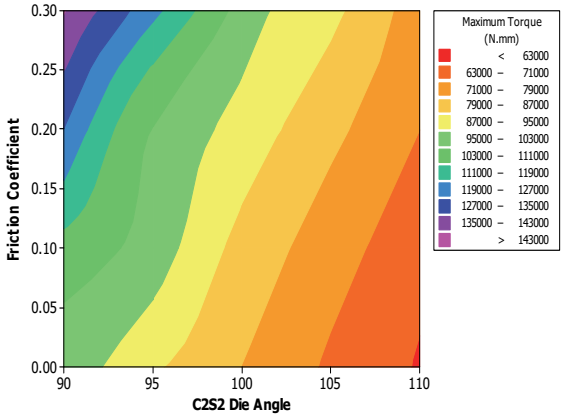

Fig. 16. Contour plot showing the effect of friction coefficient and die angle on the maximum torque needed for the execution of the C2S2 process.

4. Conclusions

In the present work, the plastic deformation characteristics of Al 1100 alloy was studied during the C2S2 process using two-dimensional elastoplastic finite element simulation and the effect of the die angle and friction coefficient is considered in the simulations. The main results are as follows:

1- The equivalent plastic strain distribution in the deformed plate is non-uniform at all frictions and C2S2 die angles. The upper sides of the samples receive more plastic strain compared with the downside regions.

2- At lower die angles, for example 90˚, the magnitude of the plastic strain at the bottom side of the sample increases by increasing the friction coefficient. But at higher die angles, for example 110˚, the friction has no significant effect on the variations of the plastic strain across the deformed plate.

3- At a constant friction coefficient, the amount of the equivalent plastic strain at a specified location across the plate decreases by increasing the C2S2 die angle.

4- The distribution pattern of the equivalent plastic strain doesn't change with the friction coefficient and C2S2 die angle.

5- The most uniform distribution of the plastic strain is achieved after deformation with a die angle of 90˚ and friction coefficient of 0.3. But deformation in the frictionless conditions using the C2S2 die angle in the range of 95-105 results in the most non-uniform plastic strain distribution.

6- The width of the deformation zone, as can be evaluated using the strain rate distribution pattern, decreases by increasing the friction coefficient and decreasing the C2S2 die angle.

7- The maximum amount of the damage factor is attained in the inner regions of the cross section of the plate during the C2S2 processing, irrespective of the magnitude of the die angle and friction coefficient, where the compressive state of stress can hinder the propagation of the initiated cracks.

8- Deformation with a friction coefficient of 0.3 and die angles of 90˚ and 110˚ is the safest condition according to the contour plot showing the distribution of the maximum damage with the die angle and friction coefficient. Besides, a higher risk of failure is encountered in the frictionless conditions and die angles in the range of 97.5-105˚.

9- The torque required to execute the C2S2 process increases by decreasing the die angle and increasing the friction coefficient.

Table 1. The C2S2 process parameters used in the finite element simulation.

Feeding roll diameter	200 mm
Feeding roll speed	0.1 rad/s
Friction coefficient between sample and die	0-0.3
Friction coefficient between sample and roller	0.9
Sample dimension	160 mm×10 mm
Material	Al 1100
C2S2 die angle	90-110˚

5. References

[1] T. Tanaka, Controlled rolling of steel plate and strip, *International of Materials Reviews*, 26 (1981) 185-212.

[2] H. Ding, N. Shen, Y. C. Shin, Predictive modeling of grain refinement during multi-pass cold rolling, *J Journal of Materials Processing Technology*, 212 (2012) 1003-1013.

[3] A. Salem, M. Glavicic, S. Semiatin, The effect of preheat temperature and inter-pass reheating on microstructure and texture evolution during hot rolling of Ti–6Al–4V, *Materials Science and Engineering A*, 496 (2008) 169-176.

[4] C. Zheng, N. Xiao, D. Li, Y. Li, Microstructure prediction of the austenite recrystallization during multi-pass steel strip hot rolling: A cellular automaton modeling, Computational Materials Science, 44 (2008) 507-514.

[5] A. P. Zhilyaev, T. G. Langdon, Using high-pressure torsion for metal processing: Fundamentals and applications, *Progress in Materials Science*, 53 (2008) 893-979.

[6] Y. Saito, H. Utsunomiya, N. Tsuji, T. Sakai, Novel ultra-high straining process for bulk materials—development of the accumulative roll-bonding (ARB) *process, Acta Materialia*, 47 (1999) 579-583.

[7] D. H. Shin, J. J. Park, Y. S. Kim, K. T. Park, Constrained groove pressing and its application to grain refinement of aluminum, *Materials Science and Engineering A*, 328 (2002) 98-103.

[8] Y. Iwahashi, J. Wang, Z. Horita, M. Nemoto, T. G. Langdon, Principle of equal-channel angular pressing for the processing of ultra-fine grained materials, *Scripta Materialia*, 35 (1996) 143-146.

[9] J. Xing, H. Soda, X. Yang, H. Miura, T. Sakai, Ultra-fine grain development in an AZ31 magnesium alloy during multi-directional forging under decreasing temperature conditions, *Materials Transactions*, 46 (2005) 1646-1650.

[10] G. Faraji, A. Babaei, M. M. Mashhadi, K. Abrinia, Parallel tubular channel angular pressing (PTCAP) as a new severe plastic deformation method for cylindrical tubes, *Materials Letters*, 77 (2012) 82-85.

[11] S. Fatemi-Varzaneh, A. Zarei-Hanzaki, Processing of AZ31 magnesium alloy by a new noble severe plastic deformation method, *Materials Science and Engineering A*, 528 (2011)1334-1339.

[12] N. Pardis, R. Ebrahimi, Deformation behavior in Simple Shear Extrusion (SSE) as a new severe plastic deformation technique, *Materials Science and Engineering A*, 527 (2009) 355-360.

[13] Q. Wang, Y. Chen, J. Lin, L. Zhang, C. Zhai, Microstructure and properties of magnesium alloy processed by a new severe plastic deformation method, *Materials Letters*, 61 (2007) 4599-4602.

[14] V. Segal, Slip line solutions, deformation mode and loading history during equal channel angular extrusion, *Materials Science and Engineering A*, 345 (2003) 36-46.

[15] Y. Miyahara, Z. Horita, T. G. Langdon, Exceptional superplasticity in an AZ61 magnesium alloy processed by extrusion and ECAP, *Materials Science and Engineering A*, 420 (2006) 240-244.

[16] X. Molodova, G. Gottstein, M. Winning, R. Hellmig, Thermal stability of ECAP processed pure copper, *Materials Science and Engineering A*, 460 (2007) 204-213.

[17] X. Zhao, X. Yang, X. Liu, X. Wang, T. G. Langdon, The processing of pure titanium through multiple passes of ECAP at room temperature, *Materials Science and Engineering A*, 527 (2010) 6335-6339.

[18] A. Zhilyaev, D. Swisher, K. Oh-Ishi, T. Langdon, T. McNelley, Microtexture and microstructure evolution during processing of pure aluminum by repetitive ECAP, *Materials Science and Engineering A*, 429 (2006) 137-148.

[19] S. Xu, G. Zhao, X. Ren, Y. Guan, Numerical investigation of aluminum deformation behavior in three-dimensional continuous confined strip shearing process, *Materials Science and Engineering A*, 476 (2008) 281-289.

[20] J. C. Lee, H. K. Seok, J. Y. Suh, Microstructural evolutions of the Al strip prepared by cold rolling and continuous equal channel angular pressing, *Acta Materialia*, 50 (2002) 4005-4019.

[21] W. Wei, W. Zhang, K. X. Wei, Y. Zhong, G. Cheng, J. Hu, Finite element analysis of deformation behavior in continuous ECAP process, *Materials Science and Engineering A*, 516 (2009) 111-118.

[22] V. P. Basavaraj, U. Chakkingal, T. P. Kumar, Study of channel angle influence on material flow and strain inhomogeneity in equal channel angular pressing using 3D finite element simulation, *Journal of Materials Processing Technology*, 209 (2009) 89-95.

[23] R. B. Figueiredo, P. R. Cetlin, T. G. Langdon, The processing of difficult-to-work alloys by ECAP with an emphasis on magnesium alloys, *Acta Materialia*, 55 (2007) 4769-4779.

[24] F. Kang, J. T. Wang, Y. Peng, Deformation and fracture during equal channel angular pressing of AZ31 magnesium alloy, *Materials Science and Engineering A*, 487 (2008) 68-73.

[25] M. S. Ghazani, B. Eghbali, Finite element simulation of cross equal channel angular pressing, Computational *Materials Science*, 74, (2013) 124-128.

[26] M. S. Ghazani, A. Vajd, Finite Element Simulation of Flow Localization during Equal Channel Angular Pressing, *Transactions of the Indian Institute of Metals*, 70 (2017) 1323-1328.

مشخصه‌های تغییرشکل فرآیند C2S2 با تأکید بر یکنواختی توزیع کرنش و تجمع فاکتور تخریب در نمونه

مهدی شبان‌قاضانی

دانشکده مهندسی، دانشگاه بناب، بناب، ایران.

چکیـــده

در تحقیق حاضر، از تحلیل المان محدود دوبعدی برای بررسی مشخصه‌های تغییر شکل آلومینیم ۱۱۰۰ درحین فرایند C2S2 استفاده شد. نتایج شبیه‌سازی‌ها نشان داد توزیع کرنش پلاستیک در نمونه تغییرشکل یافته صرف‌نظر از مقدار ضریب اصطکاک و زاویه قالب به‌صورت غیریکنواخت است. یکنواخت‌ترین توزیع کرنش در نمونه زمانی حاصل می‌شود که ضریب اصطکاک و زاویه قالب به ترتیب ۰/۳ و ۹۰ درجه درنظر گرفته شود. همچنین مشاهده شد ماکزیمم فاکتور تخریب در نواحی داخلی مقطع ورق ایجاد می‌شود که مشابه با رفتار تغییر شکل موادی با ضریب کارسختی بالا در حین پرس در کانال‌های زاویه‌دار هم مقطع می‌باشد. براساس نتایج حاصل از شبیه‌سازی با ضریب اصطکاک و زاویه قالب مختلف چنین استنباط می‌شود که مطمئن‌ترین شرایط تغییرشکل برای جلوگیری از آسیب ورق زمانی حاصل می‌شود که ضریب اصطکاک برابر با ۰/۳ و زاویه قالب ۹۰ و ۱۱۰ درجه درنظر گرفته شود. علاوه بر این با بررسی الگوی توزیع نرخ کرنش نشان داده شد که پهنای ناحیه تغییر شکل با افزایش ضریب اصطکاک و کاهش زاویه قالب کاهش پیدا می‌کند.

واژه‌های کلیدی: آنالیز المان محدود، فرایند تغییرشکل C2S2، یکنواختی کرنش پلاستیک، فاکتور تخریب.